

# Source Attribution of Black Carbon in Arctic Snow

DEAN A. HEGG\*

Department of Atmospheric Sciences, MC 351640, University of Washington, Seattle, Washington 98195

STEPHEN G. WARREN

Department of Atmospheric Sciences, MC 351640, University of Washington, Seattle, Washington 98195

THOMAS C. GRENFELL

Department of Atmospheric Sciences, MC 351640, University of Washington, Seattle, Washington 98195

SARAH J. DOHERTY

JISAO, MC 355762, University of Washington, Seattle, Washington 98195

TIMOTHY V. LARSON

Department of Civil and Environmental Engineering, MC 352700, University of Washington, Seattle, Washington 98195

ANTONY D. CLARKE

School of Ocean and Earth Sciences and Technology, University of Hawaii, Honolulu, Hawaii 96822

Received December 19, 2008. Revised manuscript received March 25, 2009. Accepted April 8, 2009.

Snow samples obtained at 36 sites in Alaska, Canada, Greenland, Russia, and the Arctic Ocean in early 2007 were analyzed for light-absorbing aerosol concentration together with a suite of associated chemical species. The light absorption data, interpreted as black carbon concentrations, and other chemical data were input into the EPA PMF 1.1 receptor model to explore the sources for black carbon in the snow. The analysis found four factors or sources: two distinct biomass burning sources, a pollution source, and a marine source. The first three of these were responsible for essentially all of the black carbon, with the two biomass sources (encompassing both open and closed combustion) together accounting for >90% of the black carbon.

## 1. Introduction

It has been realized for some time now (1–3) that the deposition of light-absorbing aerosol onto arctic snow has the potential to significantly alter the snow albedo, hence perturbing the arctic radiative balance and possibly leading to earlier snowmelt. This light-absorbing aerosol has been variously referred to as “soot”, “black carbon”, or “elemental carbon”, in large part depending on the analysis technique. In this study we use the term black carbon, consistent with its relatively broader usage and the fact that our data are derived from an optical measurement. However, note that what is given is an equivalent black carbon concentration,

derived assuming that all of the measured absorption is due to a single carbon species.

For aerosol in the arctic, there is a great deal of uncertainty and a voluminous literature on its sources, associated early on primarily with anthropogenic pollution (e.g., 4, 5). More recently, biomass burning has been recognized as an important aerosol source, particularly for black carbon (6, 7). Other aerosol sources such as the ocean (for sea salt) and biogenic emissions have also been investigated (8). Various techniques have been used to quantify the sources of arctic aerosols, including source-specific tracers (3, 9), numerical transport modeling (6), various forms of back trajectory analysis (10), and receptor modeling (8, 11). However, many of these studies did not encompass BC. Furthermore, there is a potentially substantial disjoint between source attribution of BC in atmospheric arctic aerosol and arctic snow. The latter involves—in addition to all of the factors influencing the former—such issues as scavenging efficiencies by precipitation, dry deposition rates, and the timing of precipitation events relative to inflow for the arctic region (cf., 12, 13).

Direct measurements of black carbon in arctic snow are sparse, though a number of studies have been conducted (e.g., 14–16). To date, source attribution of snow BC has relied primarily upon numerical transport modeling coupled with validation comparisons with these limited data (e.g., 9, 17). Such studies are invaluable diagnostic tools but tend to be somewhat uncertain in quantitative assessment of relative source magnitudes. To address this issue and to add to the data set on BC in arctic snow, we present a new data set on snow chemical composition and utilize these data as input to a standard receptor model to resolve the sources of the snow BC. Additionally, we test the plausibility of our source attribution using back trajectory analysis.

## 2. Experimental Methodology

**2.1. Receptor Model.** Because the source profiles, indeed, even the nature of the sources per se, are not well established for the arctic, fully deterministic modeling such as that in the well-known chemical mass balance model (e.g., (18)) cannot be employed. Instead, one must rely on various Analysis of Variance (ANOVA) approaches. These techniques employ the internal variance of chemical compositions within a sample set in the deposition (“receptor”) area to extract statistical source profiles that can then be used for source attribution. A powerful member of this family of techniques is Positive Matrix Factorization (PMF), a type of factor analysis (cf., (19)) that places various constraints on the matrix inversion (e.g., all factor loadings must be positive). Here we use the U.S. EPA version, PMF 1.1, which has been widely used in regulatory assessments.

One aspect of our application of the PMF model should be explicitly noted. Normally the model is applied to time series at a particular locale; i.e., temporal variance is analyzed. In this instance, we are treating the arctic as a receptor site whose various geographic subregions are differentially impacted by the potential sources; i.e., we are analyzing spatial variance. Such an application of ANOVA is perfectly consistent with the mathematical structure of the technique and has in fact been widely utilized by others (e.g., 20–22).

**2.2. Sample Collection.** The 36 snow samples selected for the analysis presented here were taken primarily during the spring (3 from the summer) and from close to the snow surface, typically within the first few cm but always, with the exception of the samples from Khatanga and one of the Greenland samples, within the top 20 cm of the snowpack. (The Khatanga samples extended over 34–42 cm depth and

\* Corresponding author tel: 206 685-1984; fax: 206 543-0708; e-mail: deanhegg@atmos.washington.edu.

the Greenland sample was at 40 cm.) The rationale for this approach is to confine the analysis to recently deposited aerosol particles, essentially from the current snow season, and to avoid including snow from previous years in the variance analysis. Given the climatological mean snow depth deposited per month for the winter/spring season ((23); V. Radionov, personal communication, 2008), the typical sample depths correspond to about one month's snowfall. For the Khatanga and Greenland samples, it would correspond to a bit less than two months. The snow samples were melted in the field and filtered through Nuclepore polycarbonate filters (0.4  $\mu\text{m}$  pore size) to separate out the black carbon and other water-insoluble species from the soluble analytes. Unfiltered samples were also taken and the solutes were analyzed, with no significant difference in analyte concentration found between filtered and unfiltered samples. The filtrate volumes ranged from 175 to 1300 mL and were most commonly around 300–600 mL. Aliquots of 30–80 mL were taken from the filtrate solutions, then frozen and returned to the laboratory for analysis. The filters were also returned to the laboratory for photometric and chemical composition analyses.

The sites from which samples were selected are shown in Figure S1 and listed in Table S1. The objective was to provide a reasonably representative and coherent picture of black carbon deposition for the arctic as a whole. However, by any standard, the coverage for so vast a region is sparse, with some portions of it (e.g., Eastern Siberia, Scandinavia) having no representation as yet. Hence, the analysis provided here is in no sense conclusive but should be considered exploratory though more geographically comprehensive than other such studies to date.

**2.3. Chemical Analysis.** In the laboratory, the snow filtrate aliquots were melted, treated with a biocide, and analyzed for standard anions via ion chromatography with conductivity detection (IC-COND), for carbohydrates via both liquid chromatography–mass spectroscopy (LC-MS) and IC with pulsed amperometric detection (IC-PAD), and for various elements via inductively coupled plasma–optical emission spectroscopy (ICP-OES). Details on these procedures are given in ref 24. The filters themselves were first analyzed optically for aerosol light absorption using a multiwavelength, integrating sandwich spectrophotometer similar to the one used by Clarke and Noone (2). This allows for determination of an equivalent black carbon concentration in the snow ( $\text{ng g}^{-1}$  water) assuming that all absorption is caused by black carbon and that the black carbon has a mass absorption crosssection (MAC) of  $6 \text{ m}^2 \text{ g}^{-1}$ , the crosssection of the weighed calibration standards. This may result in a high bias in derived BC where other light-absorbing aerosols (e.g., soil dust) are present (cf, (25)). Regarding MAC, the critical point is that what is actually being allocated to various sources is in fact the aerosol absorption in the snow—the key variable for radiative transfer in any case.

After the photometric analysis, the filter was extracted in 5 mL of hexane and evaporated down to 2 mL under dry nitrogen. The extracted aliquots were then analyzed for polycyclic aromatic hydrocarbons (PAHs) via gas chromatography–mass spectroscopy (GC-MS) using a C5 column as per EPA reference technique 8270.

### 3. Results and Discussion

Shown in Figure S2 are mean concentrations of black carbon and selected other chemical species (selection based on the receptor model results to be discussed below) for each of the four geographic receptor regions shown in Figure S1. Substantial geographic differences in the chemistry are apparent. For example, it is clear that the Russian sites have the highest levels of black carbon and nitrate whereas the sites near the North Pole, interestingly, have the highest non

sea salt (NSS) sulfate levels. The Greenland sites, unsurprisingly based on their high altitude and previous studies (e.g., (26)), have the lowest overall concentrations (i.e., the lowest total mass and the lowest mass for most of the individual species analyzed). Positive correlations significant at the 95% level or better were found between black carbon and a number of other species (e.g., nitrate, Al, Fe, acenaphthene). However, the linear correlation coefficient never exceeded 0.75 for any of these species and, in some cases (e.g., Fe and Al), was biased by numerous zero values. Deconvolution of the sources of the black carbon clearly requires a more sophisticated analysis, and we thus turn now to the receptor modeling.

Prior to applying the PMF model, the chemical database was assessed with regard to the reliability of the input variables. Variables for which fewer than half the sites had concentrations above the detection limit were eliminated from consideration. Those with either numerous zeros or poorer than average signal-to-noise ratios were down-weighted (by increasing the uncertainties associated with the variables by a factor of 3) to reduce their impact on the variance reduction algorithm. After taking these considerations into account, 22 chemical species were included in the receptor model (Table S2).

The model was run for 3–7 factors and always with 7 random seeds (initial starting points for the variance reduction algorithm). A choice of 4 factors gave the most stable results, and the most easily interpretable factors.  $Q$  values (modified  $\chi^2$  values) for the 4-factor solution (both robust and true) were closest to the theoretical  $Q$  value of any of the factor numbers for which the model was run, suggesting that the 4-factor solution was optimal (27). The model iteration selected for detailed analysis had a robust  $Q$  8% lower than  $Q$  theoretical. The diagnostic regression  $R^2$  for black carbon, the variable of most interest, was 0.66. While the choice of a larger factor number raised this considerably (e.g., five factor  $R^2 = 0.75$ ), the additional factors were difficult to interpret physically, being essentially fragments of factors from the lower factor number solutions with no apparent physical rationalization for the split. Therefore, the 4-factor solution is the most meaningful in terms of source identification even though higher-order solutions have a bit more prognostic power for black carbon concentrations. Diagnostic  $R^2$  values for most other key species were also reasonably high (e.g., Ca = 0.94, sulfate = 0.91, K = 0.91).

The factor loadings (apportionment of species mass to individual factors) for the 4-factor solution, essentially the source profiles, are standard outputs of the PMF 1.1 model and are given in Figure 1 (in both measured mass concentration and the % total mass allocated to each factor). The first factor or source profile (panel a) is easily interpretable. The chlorine and sodium loadings are quite high, as are those of boron, potassium, and magnesium, all sea-salt components. Furthermore, the mole ratio of chlorine to sodium is essentially that of sea salt. Hence, we interpret this factor as a marine source. The second factor (panel b) contains a very high loading of nitrate, generally indicative of combustion, coupled with high loadings of NSS potassium, succinate, oxalate, and formate, all well-known biomass-burning species. The substantial loadings of acenaphthene and pyrene are also consistent with biomass burning, though they are not unique to it. Somewhat anomalously, levoglucosan, normally an excellent tracer for biomass burning emissions, is rather modestly loaded. On the other hand, the concentration ratio of black carbon to NSS sulfate in this factor is 0.21, appreciably higher than the same concentration ratio in snow samples in which the black carbon has been attributed mostly to industrial sources (e.g., (28)). Consistent with this, the ratio is also relatively high compared to another factor (see below) that we identify with pollution (ratio of

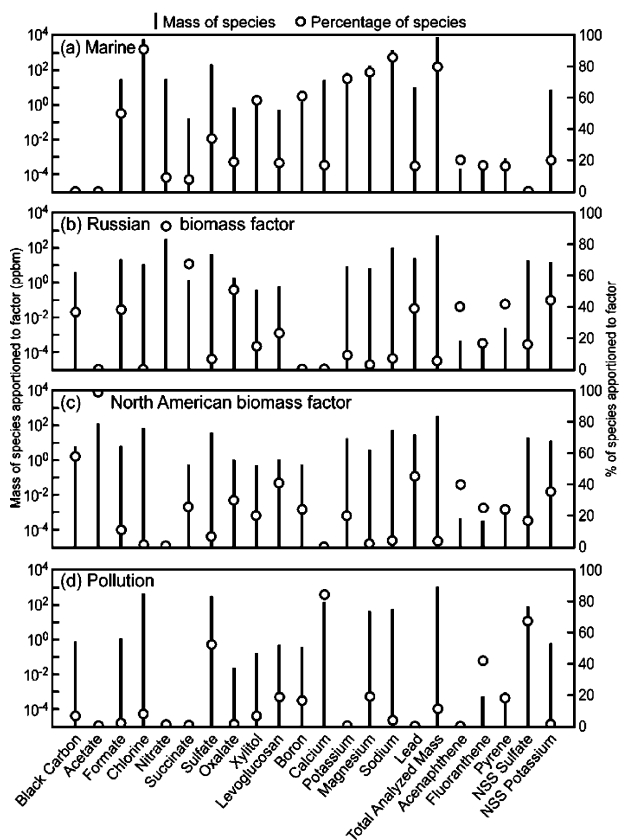


**FIGURE 1. Source profiles for the four factors/sources resolved by the PMF 1.1 model based on the chemical species listed in Table S2.**

0.01). Indeed, relatively high values of the black carbon to NSS sulfate ratio are typically found in PMF factors attributed to forest fire sources (cf., (29)). All things considered, it seems fairly clear that this source is biomass burning. However, it is also important to note that the species available do not allow us to distinguish between open and closed biomass burning sources. Sources such as residential wood burning could be substantial contributors to the biomass factors and are well-known sources in both North America and Eurasia (30). Similarly to factor two, the third PMF factor (panel c) has substantial loadings for succinate and oxalate, nearly all the acetate (another known biomass burning emission) but a less prominent loading than the second factor for NSS potassium. On the other hand, it has more levoglucosan, the most of any single factor and a black carbon to NSS sulfate ratio even higher (0.31) than that of the previous biomass-burning factor. Hence we also interpret it as a biomass source factor, noting that the second and third factors together account for over 80% of the levoglucosan mass and ~80% of the NSS potassium mass. Finally, the fourth factor (panel d) is distinguished by high loadings for sulfate, NSS sulfate, calcium, and fluoranthene. Additionally, the black carbon to NSS sulfate ratio is reminiscent of that for snow impacted mostly by industrial sources (e.g., (28)). The presence of NSS sulfate and fluoranthene would both suggest industrial pollution as well though the presence of calcium is a bit ambiguous. Normally, calcium would be considered a marker for soil but is also a well-known constituent of coal fly ash. Based primarily on the high NSS sulfate loading but also on the elevated Ca/sulfate ratio (cf., (25)), we interpret this as an anthropogenic pollution source.

While the above interpretation of the nature of the PMF factors is reasonable, there are some anomalies that need to be discussed. In preface, a cautionary note on the nature of these factors is in order. Sources identified via inverse

modeling such as PMF are not precisely the same thing as actual physical sources (e.g., a coal-fired power plant or a set of biomass fires). While the sources or factors certainly help differentiate possible physical sources, they are still a concatenation of the emissions from these sources coupled with possible differential advection, mixing with different sources, and different in situ chemistry along the trajectories. Several possible examples of this arise in the factor loadings. For example, Pb, a nearly entirely pollution-derived species, is present in all of the factors. This is not at all uncommon (e.g., (31)) and usually arises because of limited variance in the species concentration, likely due in this case to widespread diffusion of the pollution source plumes. It renders the species of little value as a source discriminant and, indeed, if Pb is removed entirely from the analysis, there is no significant difference in the results. On the other hand, some apparently discriminatory species may not be quite what they appear. For example, the major differentiating species between the two biomass factors are acetate and nitrate, the acetate loaded almost entirely onto the first biomass factor and the nitrate loaded entirely onto the second. The error analysis (by bootstrapping) shown in Figure S3 suggests that the allocation of neither species is necessarily so exclusive. Still, it is quite marked and, given that there is little if any nitrate allocated to the pollution factor, clearly not entirely physically plausible. The nitrate allocation probably reflects an artificial loading which appreciably lowered the *Q* value of the solution due to a pathological spatial variance in this species. If both acetate and nitrate are removed from the analysis, the black carbon mass is still loaded onto a single biomass factor almost exclusively (>90%). Furthermore, as discussed below, the differentiation of the biomass sources by acetate and nitrate does have some physical plausibility. Hence, although there is some uncertainty with respect to the factor interpretation, as there always is, the origin of most of the black carbon in the snow samples seems clear. About 57% of the black carbon is loaded onto the second biomass factor and about 36% is loaded onto the first biomass factor. Thus, more than 90% of the black carbon is associated with biomass burning, with the residual associated mostly with the pollution source factor. This result is somewhat surprising in that arctic aerosols have generally been considered to be largely from industrial emissions (cf., (5)) and even snowpack samples in Greenland show a major anthropogenic, industrial impact (26). On the other hand, a number of analyses (32, 33, 3) have demonstrated that for particular years and seasons (e.g., spring), biomass burning emissions can have a profound impact on the arctic aerosol and on the snow composition as well. Given this variability in the impact of particular source types, it is worthwhile to examine the source attribution of the various individual receptor sites used in the model.

Shown in Figure 2 are the contributions of each source to the individual receptor sites used in the analysis. The biomass source with the 36% black carbon loading (factor 2) is primarily associated with the Russian sites with some contribution at others (e.g., numbers 2, 8, and 11). We label it the Russian biomass factor since it is most prevalent in this receptor area—not necessarily because the actual fires that are the aerosol source are in Russia. Conversely, the second biomass source (factor 3), distinguished by the highest black carbon and acetate loadings, makes a major contribution solely at the North American sites, though it is present also at the Russian sites. We label this the North American biomass factor. The distinction between these factors, while likely at least partially artificial, is not physically implausible. Agricultural burning such as that which predominates in the spring in North America tends to be higher in acetate and lower in nitrate emissions than the mix of boreal and agricultural burning characteristic of Eurasia (33–35). Con-

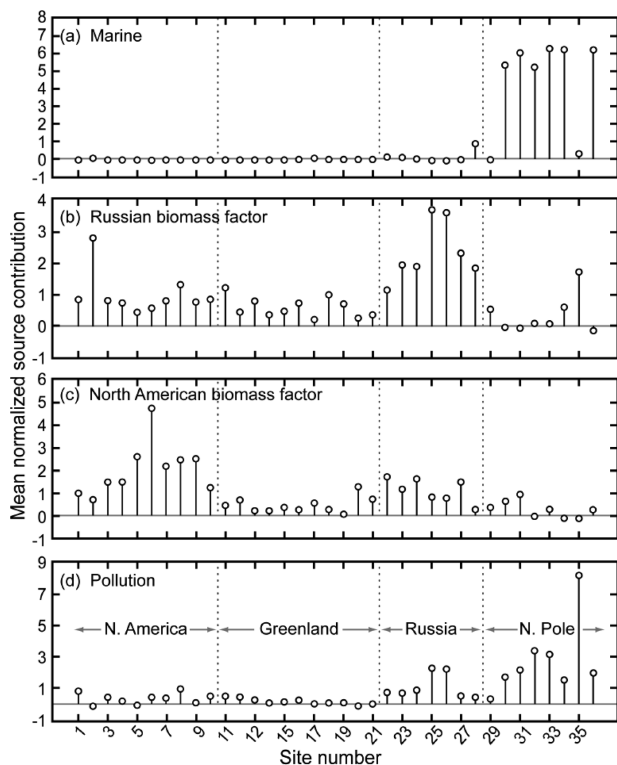


**FIGURE 2.** Contributions of each source/factor to each sample or individual receptor site. The contributions have been normalized by the average value of the respective factor contribution over all sites.

sistent with this, the black carbon to K ratio is appreciably higher (factor of 2) for the Russian as compared to the North American factor, again in accord with the boreal/agricultural dichotomy. The marine source (factor 1) is associated primarily with sea ice sites near the North Pole, again not surprisingly. However, the pollution source (factor 4) has a somewhat unexpected distribution. It has a significant presence at two of the Russian sites (25 and 26), which are near industrial emissions, but is still more significant at the North Pole sites for which the marine source is most dominant.

While interesting in itself, the contributions of the various source factors to each sample site are essentially intermediate results with regard to the main variable of interest in this study, black carbon. To arrive at the contribution of each source to the black carbon mass at each site, regressions of the black carbon mass at each site onto the normalized factor source contribution for each factor at each site (as shown in Figure 2) are made. The regression coefficients are then multiplied by the normalized source contributions to arrive at the contribution of each source to the measured black carbon mass. However, preliminary to this analysis, an assessment must be made to check the sensitivity of the factor resolution to the presence of the black carbon itself in the variable matrix. If the factors were quite sensitive to the presence of black carbon, then regression of the black carbon at the sample sites onto the corresponding factor scores becomes degenerate; i.e., we would be regressing black carbon onto what is largely a surrogate for black carbon. To ensure that this is not the case, the PMF model is rerun for precisely the same sample matrix except that black carbon is completely removed. The factor loadings for the four factors determined in these runs are then regressed, factor by factor, onto the corresponding factor loadings for the runs which include the black carbon. The  $R^2$  values from this analysis are as follows: first biomass factor = 0.9, second biomass factor = 0.99, pollution factor = 0.95, marine factor = 0.99.

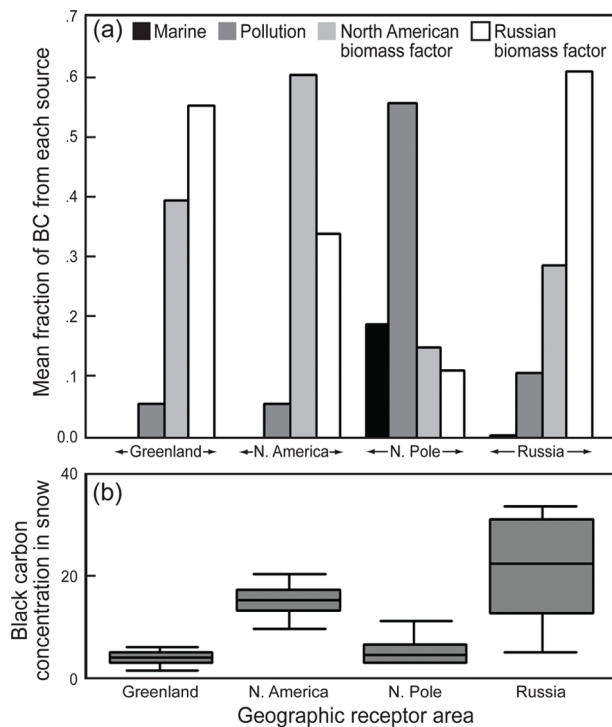


**FIGURE 3.** Results of the black carbon source allocation: (a) mean mass fraction of the black carbon in each arctic subregion or receptor area coming from each of the four source/factors; (b) absolute equivalent black carbon concentrations (ppbm) in the snow (again area means) to associate with these mass fractions. The shaded bars give the quartile range for the mean (expressed as a black line within the quartile). Error bars give the 95% range.

Hence, the factor extraction is essentially independent of the black carbon, and the regression analysis to calibrate the factor scores is valid.

The results of the black carbon attribution analysis are shown in Figure 3 in the form of the fractional contribution of the four sources to the black carbon (panel a) and the corresponding black carbon concentration in the snow (panel b). As in Figure S2, the results are shown for each of the four geographic areas for which samples were obtained. The fractional contributions are presented to more clearly show the relative impact of the sources associated with the PMF analysis. As expected, the biomass sources are the dominant contributors to the black carbon in the snow. This is true not only for the North American and Russian sites but also for Greenland, a finding in agreement with the recent analysis of McConnell and colleagues (3). Interestingly, the geographic area for which this is not the case, and for which the pollution source is dominant, is the North Pole.

To assess the possibility of long-range transport of pollution, a set of 6-day isentropic back trajectories for this receptor area was run, using the HYSPLIT IV model, over the time interval from March 16 through April 7, i.e., roughly a month before sample collection at the various sites. We use 6-day trajectories because longer trajectories show substantial instability in arctic air (36). A drawback of this is that such trajectories are commonly of insufficient length to reach source areas, though they do show directions of flow consistent with such source areas. While some of the back trajectories did impinge on the northern Siberian coast, where development is evident, by and large there was no clear, consistent pollution source revealed by this analysis. Possibly, the relatively few trajectories loosely associated with pollution are also associated with abnormally high precipitation, thus enhancing deposition to the snow. However, daily precipitation data are not available for these sites and this cannot be

corroborated. An alternative explanation would be that very local pollution from the sampling expeditions themselves had impacted the samples, though the low black carbon values suggest this is unlikely.

Back-trajectory analysis for the sites most impacted by the biomass burning factors was more broadly consistent with long-range transport of fire aerosols. For example, the Russian region, in particular the Khatanga site, not only had the highest levels of black carbon in snow of any of the sites sampled (as per Figure 3b) but also black carbon that was dominated by biomass burning emissions (as per Figure 3a). Back trajectories run from Khatanga (72.35° N, 103.18° E) between March 5 and April 14 show transport predominantly from the south, with the 6-day end points spanning a longitudinal range 60–120° E and a latitudinal range ~65–50° N. This area is close to and indeed partially overlaps the area of chronic springtime fires indicated by SPOT and MODIS burn area data over the period from 2000–2004 (37). Similar data for 2007 were supplied to us by S. Bartalev (personal communication, 2008) and suggest a source area of ~80–130° E longitude and 45–55° N latitude as do fire emission fluxes for April 2007 from FLAMBE analysis (Figure S4). While scarcely decisive, this analysis is consistent with the PMF analysis.

Another issue with interpretation of the PMF results is associated with the time of year at which the samples were obtained—from late March to early May. This period happens to coincide with that of the most intensive prescribed burning in both Siberia and the Caucasus regions. Because we generally employed samples from the topmost snow layer, representing the most recent snowfall (roughly the last 2–3 months of precipitation), it is conceivable that a temporal bias favoring the importance of biomass emissions is present in the data. In this regard, it is informative to compare the Greenland sample taken at 40 cm depth (the deepest sample analyzed) with a nearby surface sample. The surface sample has a somewhat higher total aerosol mass but is disproportionately higher in succinate, oxalate nitrate, and NSS potassium, all biomass tracers as per the above analysis. On the other hand, the NSS sulfate, a pollution marker, is disproportionately higher in the 40-cm sample. This would certainly suggest that the earlier winter snow might show a more substantial black carbon contribution from pollution. Nevertheless, most of the black carbon is in fact in the surface layer, the concentration generally decreasing with snow depth. Furthermore, it is the surface black carbon that has the most impact on the snow albedo (cf., 13, 16), the underlying motivation for this study, and it is during the spring (not winter) when reduced snow albedo has the largest climatic impact. The results presented here suggest that biomass burning is thus the largest contributor to this reduction in snow albedo in the areas and during the period we sampled.

Finally, it is important to note that the 2007 fire emissions appear to be typical, in contrast to, for example, 2003 with its very high fire incidence (37). Hence, the results presented here may be representative of more than the 2007 annual interval.

## Acknowledgments

Back trajectories used in this study were calculated with HYSPLIT-IV (HYbrid Single-Particle Lagrangian Integrated Trajectory) Model, 1997 (<http://www.arl.noaa.gov/ready/hysplit4.html>, NOAA Air Resources Laboratory, Silver Spring, MD). Annie Aggens, Stephen Hudson, Lora Koenig, James Morison, Thomas Phillips, Ron Sletten, Michael Steele, Konrad Steffen, and Matthew Sturm collected some of the snow samples used in this study. We also thank Vladimir Radionov, Valery Ippolitov, and Victor Boyarsky for logistical support in Russia. Angel Adames assisted with the spectro-

photometry, and Sergey Bartalev provided data on forest fires. Dr. Edward Hyer of NRL provided the FLAMBE data. We thank James Hansen and Ellen Baum for encouraging us to undertake this project. This work was supported by the Clean Air Task Force, the Oak Foundation, NSF Grant ARC-06-12636 and, for D.H., ONR Grant N00014-07-1-0277. Three reviewers made useful comments.

## Supporting Information Available

Locations of sample sites used in this analysis (Table S1 and Figure S1); Table S2, list of species used in the PMF analysis; Table S3, comparison of the black carbon values found in this study with some found in earlier studies; Figure S2, mean species concentrations by receptor region; Figure S3, bootstrap error analysis; and Figure S4, FLAMBE smoke data for April of 2007. This material is available free of charge via the Internet at <http://pubs.acs.org>.

## Literature Cited

- (1) Warren, S. G.; Wiscombe, W. J. Dirty snow after nuclear war. *Nature (London)* **1985**, *313*, 467–470.
- (2) Clarke, A. D.; Noone, K. J. Soot in the Arctic snowpack: a cause for perturbations in radiative transfer. *Atmos. Environ.* **1985**, *19*, 2045–2053.
- (3) McConnell, J. R.; Edwards, R.; Kok, G. L.; Flanner, M. G.; Zender, C. S.; Saltzman, E. S.; Banta, J. R.; Pasteris, D. R.; Carter, M. M.; Kahl, J. D. W. 20th-Century industrial black carbon emissions altered arctic climate forcing. *Science* **2007**, *317*, 1381–1384.
- (4) Sturges, W.; Barrie, L. Stable lead isotope ratios in Arctic aerosols: evidence for the origin of Arctic air pollution. *Atmos. Environ.* **1989**, *23*, 2513–2520.
- (5) Maenhaut, W.; Cornille, P.; Pacyna, J.; Vitols, V. Trace element composition and origin of the atmospheric aerosol in the Norwegian Arctic. *Atmos. Environ.* **1989**, *23*, 2551–2570.
- (6) Stohl, A. Pan-arctic enhancements of light absorbing aerosol concentrations due to North American boreal forest fires during summer 2004. *J. Geophys. Res.* **2006**, *111*, doi: 10.1029/2006JD007216.
- (7) Koch, D.; Hansen, J. Distant origins of Arctic black carbon: a Goddard Institute for Space Studies Model-E Experiment. *J. Geophys. Res.* **2005**, *110*, doi: 10.1029/2004JD005296.
- (8) Xie, Y.-L.; Hopke, P. K.; Paatero, P.; Barrie, L. A.; Li, S.-M. Identification of source nature and seasonal variations of Arctic aerosol by positive matrix factorization. *J. Atmos. Sci.* **1999**, *56*, 249–260.
- (9) Rahn, K. A.; Lowenthal, D. Elemental tracers of distant regional pollution aerosols. *Science* **1984**, *223*, 132–139.
- (10) Sharma, S.; Andrews, E.; Barrie, L.; Ogren, J.; Lavoue, D. Variations and sources of equivalent black carbon in the high Arctic revealed by long-term observations at Alert and Barrow: 1989–2003. *J. Geophys. Res.* **2006**, *111*, doi: 10.1029/2005JD006581.
- (11) Polissar, A.; Hopke, P.; Malm, W.; Sisler, J. Atmospheric aerosol over Alaska I. Elemental composition and sources. *J. Geophys. Res.* **1998**, *103*, 19045–19057.
- (12) Rahn, K. A.; McCaffrey, R. J. Long-range transport of pollution aerosol to the Arctic: A problem without borders. *Corros. Sci.* **1979**, *25*–35.
- (13) Flanner, M. G.; Zender, C. S.; Randerson, J. T.; Rasch, P. J. Present-day climate forcing and response from black carbon in snow. *J. Geophys. Res.* **2007**, *112*, doi: 1029/2006JD008003.
- (14) Peters, A.; Teixeira, C.; Jones, N.; Spencer, C. Recent depositional trend of polycyclic aromatic hydrocarbons and elemental carbon to the Agassiz ice cap. *Sci. Total Environ.* **1995**, *167*–175.
- (15) Masclat, P.; Hoyau, V.; Jaffrezo, J.; Cachier, H. Polycyclic aromatic hydrocarbon deposition on the ice sheet of Greenland. Part I: superficial snow. *Atmos. Environ.* **2000**, *34*, 3195–3207.
- (16) Grenfell, T. C.; Light, B.; Sturm, M. Spatial distribution and radiative effects of soot in the snow and sea ice during the SHEBA experiment. *J. Geophys. Res.* **2002**, *107*, doi: 10.1029/2000JC000414.
- (17) Generoso, S.; Bey, I.; Attie, J.-L.; Breon, F.-M. A satellite- and model-based assessment of the 2003 Russian fires: impact on the Arctic region. *J. Geophys. Res.* **2007**, *112*, doi: 10.1029/2006JD008344.
- (18) Hidy, G.; Venkataraman, C. The chemical mass balance method for estimating atmospheric particle sources in Southern California. *Chem. Eng. Commun.* **1996**, *151*, 187–209.

- (19) Paatero, P.; Tapper, U. Positive matrix factorization: a non-negative factor model with optimal utilization of error estimates of data values. *Environmetrics* **1994**, *5*, 111–126.
- (20) Reimann, C.; Fitzmoser, P.; Garrett, R. Factor analysis applied to regional geochemical data: problems and possibilities. *Appl. Geochem.* **2002**, *17*, 185–206.
- (21) Paatero, P.; Hopke, P.; Hoppenstick, J.; Eberly, S. Advanced factor analysis of spatial distributions of PM<sub>2.5</sub> in the Eastern United States. *Environ. Sci. Technol.* **2003**, *37*, 2460–2476.
- (22) Chen, L.-W.; Watson, J.; Chow, J.; Magliano, K. Quantifying PM<sub>2.5</sub> source contributions for the San Joaquin Valley with multivariate receptor models. *Environ. Sci. Technol.* **2007**, *41*, 2818–2826.
- (23) Adam, J. C.; Lettenmaier, D. P. Application of new precipitation and reconstructed streamflow products to streamflow trend attribution in Northern Eurasia. *J. Climate* **2008**, *21*, 1807–1828.
- (24) Gao, S.; Hegg, D.; Hobbs, P.; Kirchstetter, T.; Magi, B.; Sadelik, M. Water-soluble organic components in aerosols associated with savanna fires in southern Africa: identification, evolution and distribution. *J. Geophys. Res.* **2003**, *108*, doi: 10.1029/2002JD002324.
- (25) Clarke, A. Biomass burning and pollution aerosol over North America: organic components and their influence on spectral optical properties and humidification response. *J. Geophys. Res.* **2007**, *112*, doi: 10.1029/2006JD007777.
- (26) Davidson, C.; Harrington, J.; Stephenson, M.; Small, M.; Boscoe, F.; Gandley, R. Seasonal variations in sulfate, nitrate and chloride in the Greenland ice sheet. Relation to atmospheric concentrations. *Atmos. Environ.* **1989**, *23*, 2483–2493.
- (27) Reff, A.; Eberly, S. I.; Bhave, P. Receptor modeling of ambient particulate matter data using Positive Matrix Factorization: review of existing methods. *J. Air Waste Manage. Assoc.* **2007**, *57*, 146–154.
- (28) Noone, K.; Clarke, A. Soot scavenging measurements in the arctic snowfall. *Atmos. Environ.* **1988**, *22*, 2773–2778.
- (29) Polissar, A. V.; Hopke, P. K.; Paatero, P.; Malm, W. C.; Sisler, J. F. Atmospheric aerosol over Alaska 2. Elemental composition and sources. *J. Geophys. Res.* **1998**, *103*, 19045–19057.
- (30) Bond, T. C.; Streets, D. G.; Yarber, K. F.; Nelson, S. M.; Woo, J.-H.; Klimont, Z. W. A technology-based global inventory of black and organic carbon emissions from combustion. *J. Geophys. Res.* **2004**, *109*, doi: 10.1029/2003JD003697.
- (31) Anttila, P.; Makkonen, U.; Hellen, H.; Kyllonen, K.; Leppanen, H. S.; Hakola, H. Impact of open biomass fires in the spring and summer of 2006 on the chemical composition of background air in south-eastern Finland. *Atmos. Environ.* **2008**, *42*, 6472–6486.
- (32) Stohl, A., et al. Pan-Arctic enhancements of light absorbing aerosol concentrations due to North American boreal forest fires during summer 2004. *J. Geophys. Res.*, **2006**, *111*, doi: 10.1029/2006JD007216.
- (33) Warneke, C., et al. Biomass burning in Siberia and Kazakhstan as an important source for haze over the Alaskan Arctic in April 2008. *Geophys. Res. Lett.* **2009**, *36*, doi: 10.1029/2008GL036194.
- (34) Hays, M. D.; Geron, C. D.; Linna, K. J.; Smith, N. D.; Schaur, J. J. Speciation of gas-phase and fine particle emissions from burning of foliar fuels. *Environ. Sci. Technol.* **2003**, *36*, 2281–2295.
- (35) Hays, M. D.; Fine, P. M.; Geron, C. D.; Kleeman, M. J.; Gullett, B. K. Open burning of agricultural biomass: physical and chemical properties of particle-phase emissions. *Atmos. Environ.* **2005**, *39*, 6747–6764.
- (36) Brock, C. A. Microphysical, chemical and meteorological aspects of aerosol hazes in the arctic. PhD Dissertation, University of Washington, Seattle, WA, 1990.
- (37) Bartalev, S. A.; Egorov, V. A.; Loupian, E. A.; Uvarov, I. A. Multi-year circumpolar assessment of the area burnt in boreal ecosystems using SPOT-Vegetation. *Int. J. Remote Sensing* **2007**, *28*, 1397–1404.

ES803623F

Supporting Information for

**SOURCE ATTRIBUTION OF BLACK CARBON IN ARCTIC SNOW**

by

Dean A. Hegg, Stephen G. Warren, Thomas C. Grenfell, Sarah J. Doherty,  
Timothy V. Larson and Antony D. Clarke

([deanhegg@atmos.washington.edu](mailto:deanhegg@atmos.washington.edu))

This SI is five pages long, including the cover page, and contains three tables and four figures.

Table S1. Locations of sampling sites used in the analysis. Samples 16 and 20 are summer samples (removed in a sensitivity study).

Site number	Region	Latitude	Longitude	Name
1	North America	65 36.4 N	122 15.6 W	Sturm traverse
2	North America	65 57.4 N	112 25.3 W	Sturm traverse
3	North America	66 13.8 N	121 3.9 W	Sturm traverse
4	North America	67 9.6 N	130 15.4 W	Sturm traverse
5	North America	67 34.1 N	138 17.9 W	Sturm traverse
6	North America	66 15.3 N	144 46.1 W	Sturm traverse
7	North America	64 56.0 N	124 46.5 W	Sturm traverse
8	North America	63 36.6 N	105 7.69 W	Sturm traverse
9	North America	64 34.6 N	98 33 W	Sturm traverse
10	North America	64 25.1 N	96 25.3 W	Sturm traverse
11	Greenland	81 N	59 W	Petermann
12	Greenland	77.45 N	60.5 W	GITS
13	Greenland	67.0 N	43.0 W	NASA-SE
14	Greenland	66.4 N	44.5 W	Saddle
15	Greenland	67.0 N	46.0 W	Dye 2
16	Greenland	67.0 N	46.0 W	Dye 2
17	Greenland	76.4 N	67.7 W	Thule
18	Greenland	72.6 N	38.5 W	Summit
19	Greenland	72.6 N	38.5 W	Summit
20	Greenland	67.0 N	46.0 W	Dye 2
21	Greenland	63.25 N	44.5 W	South Dome
22	Russia	67.6 N	53.2 E	Nar'yan Mar
23	Russia	67.6 N	53.2 E	Nar'yan Mar
24	Russia	67.6 N	53.2 E	Nar'yan Mar
25	Russia	72.4 N	103.3 E	Khatanga
26	Russia	72.4 N	103.3 E	Khatanga
27	Russia	72.4 N	103.3 E	Khatanga
28	Russia	73.4 N	81.4 E	Dikson
29	Russia	73.4 N	81.4 E	Dikson
30	N. Pole	88.1 N	90.72 W	Steele camp
31	N. Pole	89.2 N	102.5 W	Steele camp
32	N. Pole	89.4 N	0.07 W	Aggens camp
33	N. Pole	89.7 N	22.4 W	Aggens camp
34	N. Pole	89.5 N	0.66 W	Aggens camp
35	N. Pole	89.3 N	1.03 W	Aggens camp
36	N. Pole	89.9 N	30.6 W	Aggens camp

Table S2. Chemical species used in the PMF analysis together with their concentration means and ranges (ppbm) in the data set.

Species	minimum	maximum	mean	Std Dev
Black carbon	1.0	69.	12.5	13.9
Acetate	0	1340	146	251
Formate	0	346	51.7	77.9
Chloride	13.	35760	5850	12200
Nitrate	50.	1130	320	272
Succinate	0	37.	4.6	9.1
Sulfate	29.	3390	629	847
Oxalate	0	25.	4.0	6.0
Xylitol	0	13	2.1	3.4
Levogluconan	1.1	12	4.0	2.3
Boron	0	14.	2.1	3.5
Calcium	0	1650	166	314
Potassium	10	580	87.8	142
Magnesium	0	1730	224	448
Sodium	40	11700	1540	3060
Lead	0	237	65.2	63.2
Total analyzed mass	352.	48800	9120	16500
Acenaphthene	0	0.006	0.001	0.001
Fluoranthene	0	0.009	0.001	0.0025
Pyrene	0	0.02	0.006	0.0047
NSS Sulfate	0	1910.	259	392
NSS_Potassium	5.6	114	29.9	27.1

Table S3. Comparison of black carbon concentrations measured in this study with selected previous measurements. Values are data set medians in ppbm.

Region	Clarke and Noone, 1983-1984 (2)	Grenfell et al, 1998 (16)	This work, 2007
Arctic Ocean	32	4	4
Russia	-	-	22
Greenland	2	-	4
Canada	21	-	15

Figure S1 The distribution of sampling sites. Black open dots are the sampling sites. The four boxes show the receptor regions. Aggens Camp and Steele Camp sites are contained in the box around the North Pole.

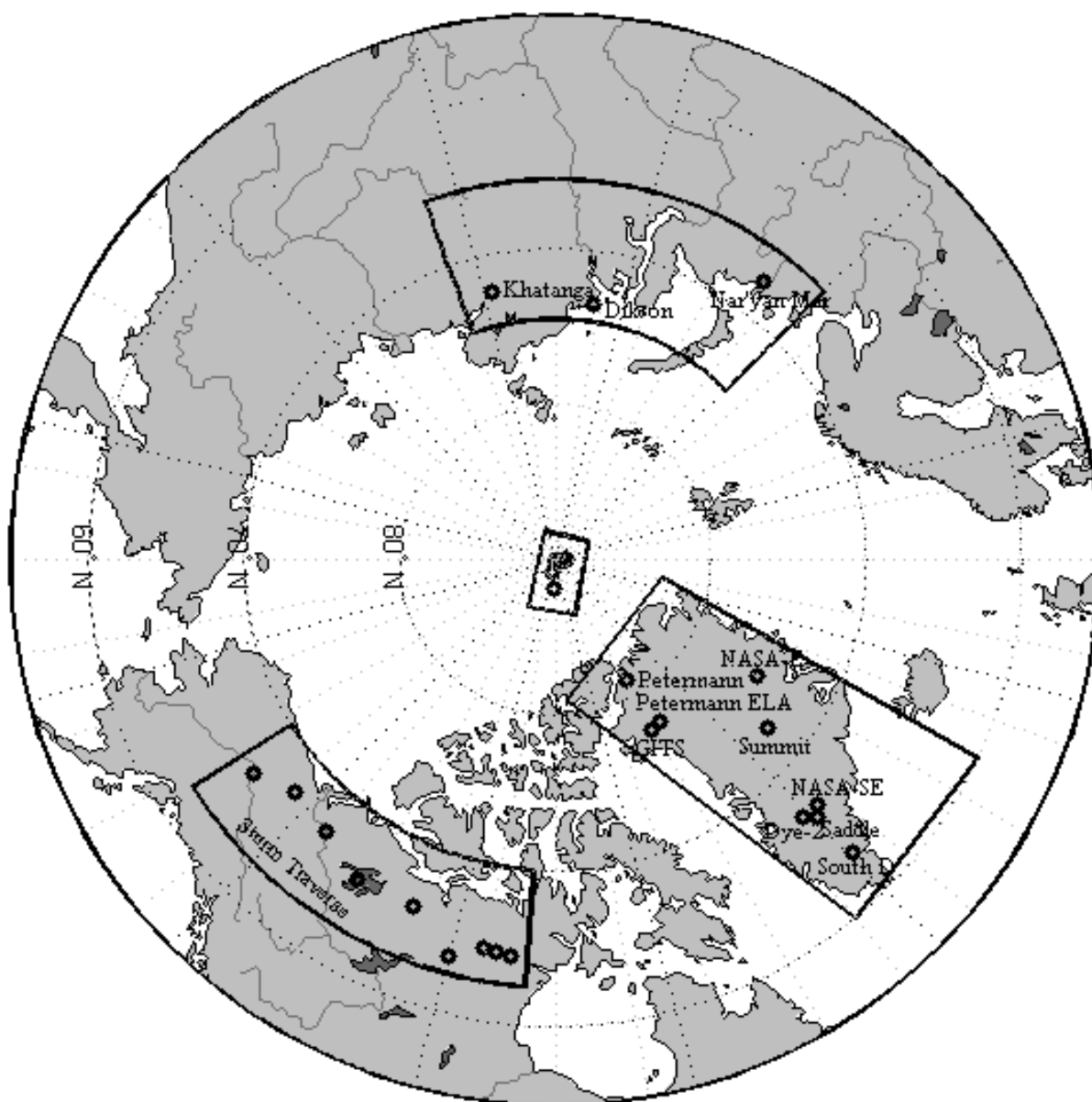


Figure S2. Mean concentrations of selected chemical species for the four sub-regions of the arctic shown in Figure S1. Panel (a) gives the actual concentrations in snow (ppbm) while Panel (b) is based on the same data but normalizes each chemical species by the maximum regional mean value for that species over all four regions. This normalization facilitates intra-species comparison between regions since bar lengths are now on a linear scale.

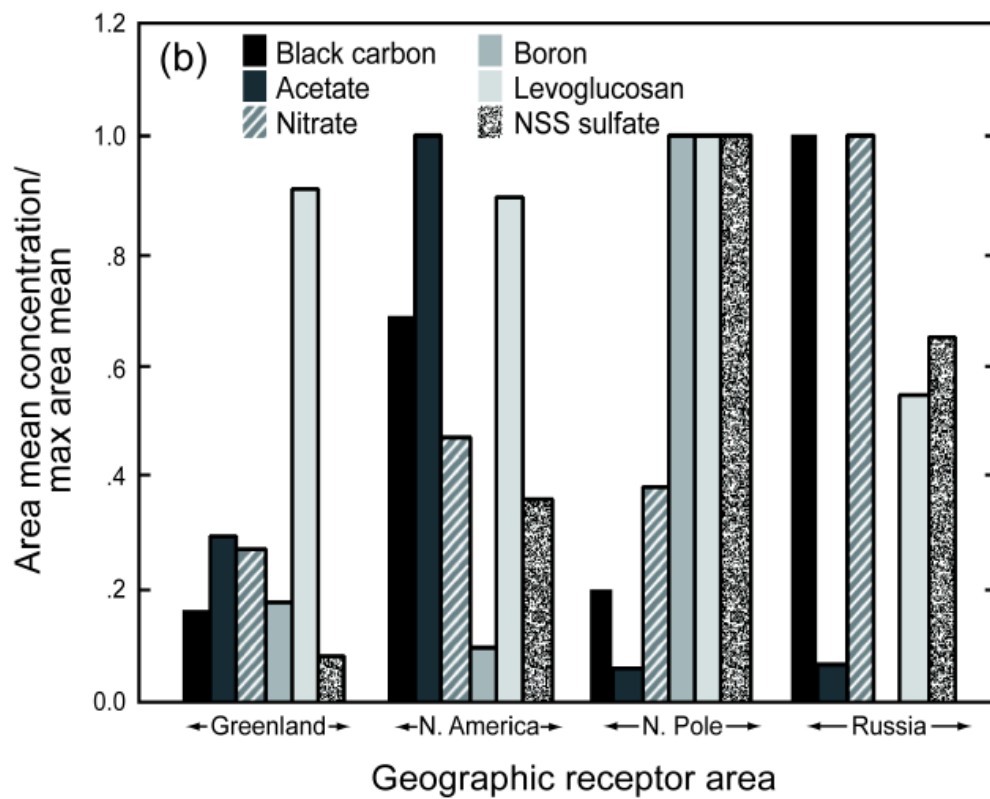
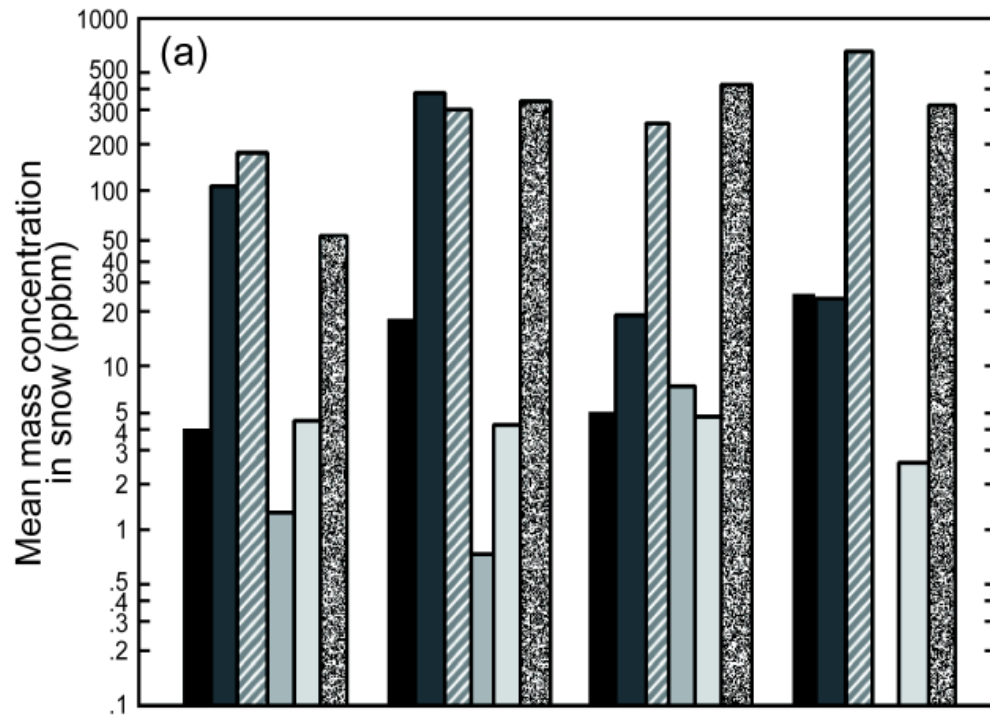


Figure S3. Results of the bootstrap uncertainty analysis (1) of the factor loadings for the four factor solution.

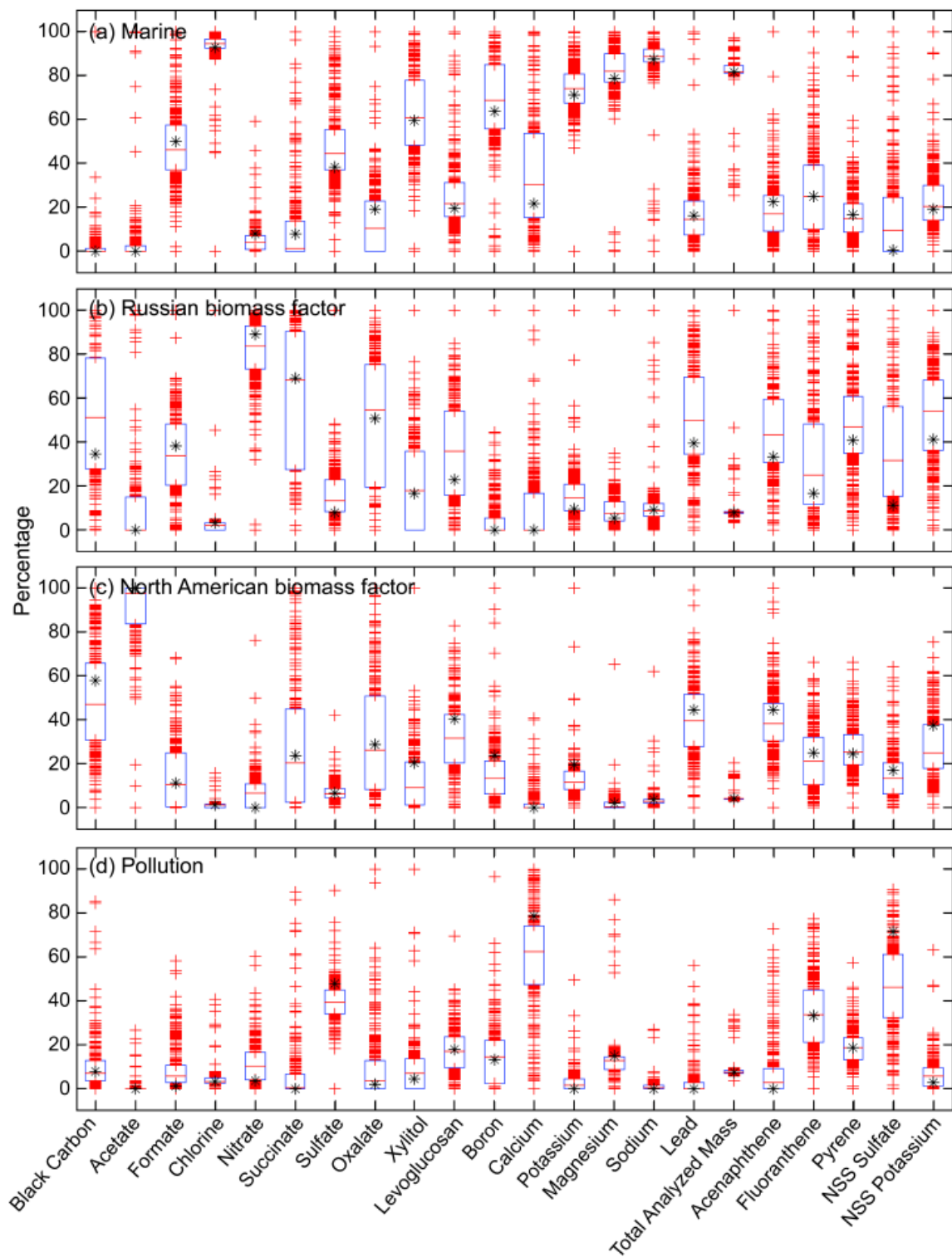
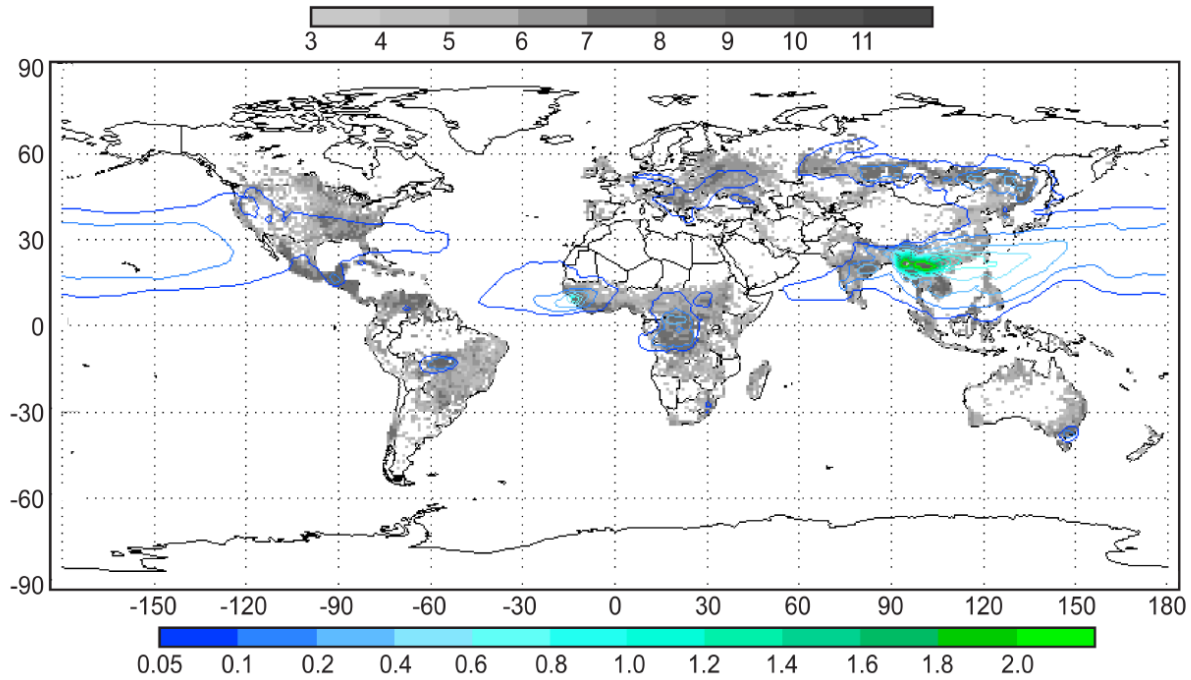


Figure S4 Geographic distribution of smoke emissions from FLAMBE for April, 2007. Gray scale gives the emissions in terms of base 10 log of kg/ 6 hrs, as do the interpolated isopleths (in color).



## References

(1) Wisnowski, J.W.; Simpson, J.R.; Montgomery, D.C.; Runger, G.C. Resampling methods for variable selection in robust regression. *Computational Statistics and Data analysis*, **2003**, 43, 341-355.